

## Steady-State Microwave Mode Cooling with a Diamond N-V Ensemble

Donald P. Fahey<sup>1,\*</sup>, Kurt Jacobs<sup>1,2</sup>, Matthew J. Turner<sup>3,4</sup>, Hyeonrak Choi<sup>5</sup>, Jonathan E. Hoffman<sup>1</sup>, Dirk Englund<sup>5</sup> and Matthew E. Trusheim<sup>1,5,†</sup>


<sup>1</sup>*DEVCOM Army Research Laboratory, Sensors and Electron Devices Directorate, Adelphi, Maryland 20783, USA*

<sup>2</sup>*Department of Physics, University of Massachusetts at Boston, Boston, Massachusetts 02125, USA*

<sup>3</sup>*Quantum Technology Center, University of Maryland, College Park, Maryland 20742, USA*

<sup>4</sup>*Department of Electrical and Computer Engineering, University of Maryland, College Park, Maryland 20742, USA*

<sup>5</sup>*Department of Electrical Engineering and Computer Science, Massachusetts Institute of Technology, 77 Massachusetts Avenue, Cambridge, Massachusetts 02139, USA*

 (Received 24 October 2022; revised 7 February 2023; accepted 8 February 2023; published 17 July 2023)

A fundamental result of quantum mechanics is that the fluctuations of a bosonic field are given by its temperature  $T$ . An electromagnetic mode with frequency  $\omega$  in the microwave band has a significant thermal photon occupation at room temperature according to the Bose-Einstein distribution  $\bar{n} = k_B T / \hbar \omega$ . The room-temperature thermal state of a  $(2\pi \times 3)$ -GHz mode, for example, is characterized by a mean photon number  $\bar{n} \sim 2000$  and variance  $\Delta n^2 \approx \bar{n}^2$ . This thermal variance sets the measurement noise floor in applications ranging from wireless communications to positioning, navigation, and timing to magnetic resonance imaging. We overcome this barrier in continuously cooling a  $(2\pi \times 2.87)$ -GHz cavity mode by coupling it to an ensemble of optically spin-polarized nitrogen-vacancy (N-V) centers in a room-temperature diamond. The N-V spins are pumped into a low entropy state via a green laser and act as a heat sink to the microwave mode through their collective interaction with microwave photons. Using a simple detection circuit, we report a peak noise reduction of  $-2.3 \pm 0.1$  dB and minimum cavity mode temperature of  $150 \pm 5$  K. We also present a linearized model to identify the important features of the cooling, and demonstrate its validity through magnetically tuned, spectrally resolved measurements. The realization of efficient mode cooling at ambient temperature opens the door to applications in precision measurement and communication, with the potential to scale towards fundamental quantum limits.

DOI: [10.1103/PhysRevApplied.20.014033](https://doi.org/10.1103/PhysRevApplied.20.014033)

### I. INTRODUCTION

Traditional methods of thermal noise reduction in the microwave regime have relied on cooling the entire apparatus [1–4]. A more direct route is to cool the electromagnetic modes themselves. This is possible when a single mode in a cavity has a very low heat capacity and long thermalization time compared with the constituent material. Targeted cooling of a subsystem has long been employed in atomic gases [5,6], trapped ions [7,8], and micromechanical oscillators [9,10], but only recently has the selective cooling of an electromagnetic mode of interest been explored. In Wu *et al.* [11], the effectively low temperature of a polarized spin bath of pentacene was used to remove the thermal energy from a cavity mode through their mutual coupling, but was limited to pulsed

operation. A recent demonstration with diamond nitrogen vacancy centers showed cooling down to 188 K from room temperature with 10-ms pulses [12]. In this work, we extend this to fully continuous microwave cavity mode cooling and explain its mechanism with an analytic theory. Our quantum mechanical treatment of this “spin refrigerator” indicates an optimal parameter regime that depends both on cavity coupling parameters and spin ensemble inhomogeneity.

We consider the system presented schematically in Fig. 1. Here a microwave mode is confined within a dielectric resonator, where it couples to the nitrogen-vacancy (N-V) spin ensemble in a colocated diamond via magnetic dipole interaction  $H_{\text{int}} = -\hat{\mu} \cdot \hat{B}$ , where  $\hat{\mu}$  is the transition (magnetic) dipole moment and  $\hat{B}$  is the magnetic field operator of the cavity mode [13]. The negatively charged N-V center possesses a triplet ground state with spin transition  $m_s = 0 \leftrightarrow m_s = \pm 1$  at  $2\pi \times 2.87$  GHz and 290 K. An external magnetic bias field breaks the degeneracy of

\*donaldpfahey@gmail.com

†mtrush@mit.edu

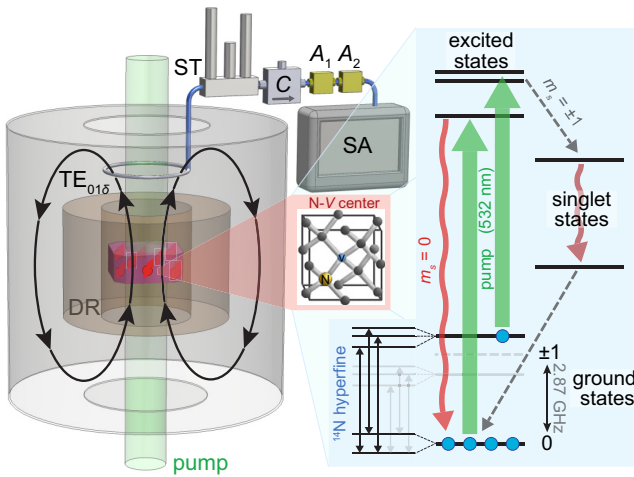


FIG. 1. Cooling a microwave mode with a diamond N- $V$  ensemble: a purple diamond inside a dielectric resonator (DR) at room temperature is pumped with a green laser. The hyperpolarized N- $V$  ground-state spins are coupled to the  $TE_{01\delta}$  cavity mode by shifting them into resonance with magnetic bias coils (not shown). The resulting reduction in mode temperature is probed by a coupling loop and spectrum analyzer (SA) via a stub tuner (ST), circulator (C), and two stage amplifiers ( $A_1$  and  $A_2$ ).

the  $m_s = \pm 1$  N- $V$  ground-state spin levels and tunes one of the spin transitions near resonance with the microwave mode. Simultaneously, each N- $V$  center undergoes spin polarization under off-resonant laser illumination via the excited orbital state and subsequent intersystem crossing and relaxation [14]. This process, in competition with direct spin relaxation, produces a net steady-state polarization, equivalent to a low-temperature N- $V$  spin population. The coupling to the microwave resonator transfers thermal excitations in the cavity mode to the cold spin bath.

Our experimental approach uses a microwave cavity consisting of two cylindrical stacked dielectric resonators inside a conductive (aluminum) cylindrical shell [15]. The resonator halves are made of high dielectric constant, low-loss ceramic sandwiched around a silicon carbide (SiC) substrate supporting the  $(3 \times 3 \times 0.9)$ -mm<sup>3</sup> CVD-grown diamond sample with 4 ppm total nitrogen-vacancy center concentration [16]. The  $TE_{01\delta}$  mode, chosen for its spatial uniformity and spectral separation from nearby modes, is probed with a shorted loop positioned above the resonator. A high-power 532-nm pump laser, left on throughout the experiment, continuously polarizes the ground state of the diamond N- $V$  ensemble spins. Cavity mode cooling due to the strong coupling to these polarized spins is observed when the N- $V$  spins are Zeeman shifted into resonance with the cavity mode by way of an applied magnetic field. We develop a theoretical analysis to better understand the nature of this cooling and test it against a range

of experimental parameters, both of which are presented below.

## II. MODEL

For a polarized spin ensemble in the weak-excitation limit, where the mean intracavity photon number  $\bar{n}$  normalized by the number of cavity-coupled N- $V$  centers ( $N$ ) is small,  $\bar{n}/N \sim 0$ , we can approximate the spins as harmonic oscillators [17]. This ‘linearized’ approach, also called the Dicke or Tavis-Cummings model [18], has been widely used for describing the coupling between spin ensembles and the cavity mode. Cavity mode cooling in this approximation can be understood following the quantum Langevin equation [19–21]. The interaction of a system with a bath of harmonic oscillators (spins) that has a Lorentzian distribution of frequencies can be described exactly by an interaction with a single-spin pseudomode that is itself damped by coupling to the standard Markovian thermal bath of oscillators [22,23]. The rate at which this single pseudomode is damped to the Markovian bath is given by the frequency spread of the original spin bath. Since the decoherence rate of the N- $V$  centers and the damping rate (polarization rate) per N- $V$  center provided by the pump laser are small compared to the inhomogeneous broadening, it is the latter that provides the irreversible damping of the spin system to the cold bath.

We parametrize the system in a linear model following the prescription above: using the collective interaction rate between the cavity and the spins,  $g$ , the internal loss rate and the output coupling rate of the cavity mode, respectively denoted by  $\gamma$  and  $\kappa$  (and through which the cavity mode is heated by a room-temperature bath), the inhomogeneous broadening of the N- $V$  ensemble,  $r$ , and the polarization  $P = |P_0 - P_1|$  of the spin bath provided by the continual laser pumping, where  $P_0$  ( $P_1$ ) is the population of  $m_s = 0$  ( $1$ ) normalized by the total number of N- $V$  centers in either  $m_s = 0$  or  $m_s = 1$  states. We give the main results of our linear model here, while the full theoretical analysis is given in the Supplemental Material [24].

The mean intracavity photon number  $\bar{n}$  evaluates to a weighted sum of the room-temperature photon number  $n_T = [\exp(\hbar\omega/k_B T) - 1]^{-1}$  and the effective ‘cold spin bath’ photon number  $n_c = (1/2)[(1 - P)/P]$ :

$$\bar{n} = \cos^2(\theta)n_T + \sin^2(\theta)n_c. \quad (1)$$

Here  $\sin^2(\theta) \equiv \xi r / (\kappa + \gamma + \xi r)$  denotes the ‘cooling ratio’ under an effective cooling rate  $\xi r$ . This rate is the inhomogeneous broadening of the spins reduced by the dimensionless parameter  $\xi = (1 + [r(r + \kappa + \gamma)/4g^2])^{-1}$ . Highly effective cooling is obtained when  $r \gg \kappa + \gamma$  and  $g \gtrsim r$ . In particular, the theory reveals that it is the inhomogeneous broadening of the ensemble, along with the ensemble coupling  $g$ , that primarily governs the rate at

which heat is extracted from the ensemble. The per-spin polarization rate  $\Gamma_p$  induced by the laser only determines the temperature of the spin bath rather than the rate of extraction of thermal power, and as such, can be much smaller than  $r$  and  $g$ .

$$N_P(\omega) = n_T + (n_c - n_T) \left[ \frac{\kappa r g^2}{(r^2/4 + \omega^2)[(\kappa + \gamma)^2/4 + (\omega - \Delta)^2] + g^2[r(\kappa + \gamma)/2 - 2\omega(\omega - \Delta)] + g^4} \right], \quad (2)$$

where  $\omega = 0$  is the cavity frequency and  $\Delta$  gives the cavity-spin detuning. When the spins are resonant, the frequency at which the noise reduction is maximal occurs at the cavity frequency unless  $8g^2 > r^2 + (\kappa + \gamma)^2$ , in which case the maximum happens for  $\omega^2 = g^2 - [r^2 + (\kappa + \gamma)^2]/8$ . In the former case the maximum noise reduction is  $2\kappa r g^2(n_T - n_c)/[4g^2 + r(\kappa + \gamma)]^2$  and in the latter it is  $64\kappa r g^2(n_c - n_T)/[(\gamma + \kappa + r)^2(16g^2 - (\gamma + \kappa - r)^2)]$ .

In principle, the ultimate limit for cooling the cavity mode is the temperature of the spin ensemble, which is exceedingly low even for modest spin polarizations (e.g., 340 mK for  $P = 0.2$  and  $\omega = 2\pi \times 2.87$  GHz). Accounting for practical limits on spin-cavity coupling  $g$  and cavity quality factor  $Q$  (which determines  $\gamma$ ), a few Kelvin-mode temperatures are still achievable. To visualize this, we have numerically minimized the noise power in Eq. (2) over a range of  $g$  and  $Q$  for the case of  $P = 0.8$ ,  $r = g$ , and cavity mode frequency  $\omega = 2\pi \times 2.87$  GHz. The linear model predictions shown in Fig. 2 indicate the potential for cryogenic-level cooling with about megahertz-scale coupling and quality factors of a few tens of thousand.

### III. METHODS

A simplified depiction showing the basic features of our setup is shown in Fig. 1. The diamond is centered inside a microwave resonator consisting of two dielectric cylindrical pucks with a center bore to provide space for the diamond as well as optical access. The resonator material and dimensions are similar to those in Ref. [15] and resulted in a  $TE_{01\delta}$  mode near the diamond N- $V$  zero-field splitting of  $\omega = 2\pi \times 2.87$  GHz.

The purple diamond ( $3 \times 3 \times 0.9$  mm<sup>3</sup>, N- $V > 4$  ppm) is situated on a 330- $\mu$ m-thick, two-inch diameter SiC wafer (4H semi-insulating, MSE Supplies) that provides a thermally conductive path to a surrounding aluminum shield. This shield provides both a heat sink for the diamond and mode confinement for the microwaves. Pump light is provided by a diode-pumped solid-state laser providing up to 10 W of continuous-wave power at 532 nm

The electromagnetic mode temperature is obtained through the noise power spectrum. The reduction in temperature depends on the measured electromagnetic mode frequency as well as the spin-cavity detuning. The linear theory gives the cavity output power spectrum as

(Lighthouse Photonics Sprout-G), and its intensity is controlled with a motorized laser power attenuator (Optogama LPA). The beam is expanded to a  $1/e^2$  diameter of 5 mm to improve the pump homogeneity across the sample, and apertured to a 6.5 mm diameter to avoid unwanted heating from beam edges. A dichroic mirror is used as the last reflector before the microwave shield to allow for the collection of photoluminescence for optically detected magnetic resonance (ODMR) and microwave-assisted charge state spectroscopy [25]. This *in situ* ODMR is used for the diamond cavity system to calibrate between N- $V$  spin shift values for a given Helmholtz coil bias current.

The cavity mode is probed with a shorted 6-mm diameter loop formed from the center conductor of one end of a 10-cm piece of coaxial cable (Pasternack RG405,

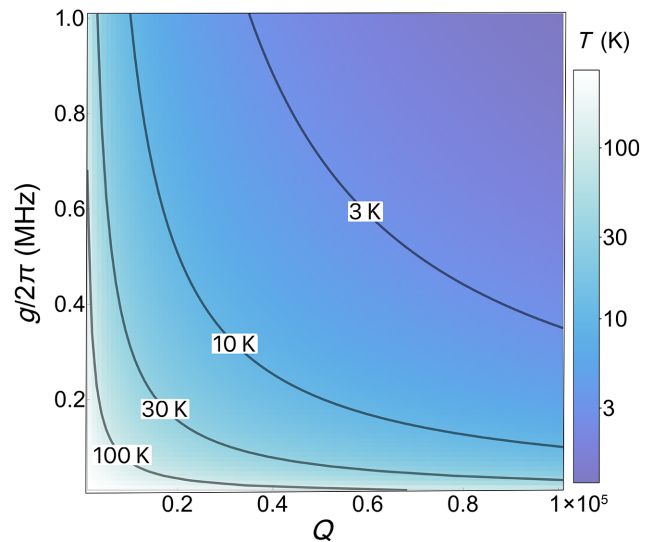


FIG. 2. Minimum cavity mode temperatures predicted by the linear model [Eq. (2)] for a range of spin-cavity couplings and cavity  $Q = \omega/\gamma$ ,  $\omega = 2\pi \times 2.87$  GHz (i.e., diamond N- $V$  centers),  $r = g$ , and spin polarization  $P = 0.8$ , showing that temperatures competitive with cryogenic systems should be achievable with experimentally feasible quality factors and sufficiently strong coupling.

0.5-dB loss per foot), and concentrically aligned with the dielectric resonator 6 mm from one end. The loop feed is connected to a three-stub tuner (Maury Microwave) and a low-loss circulator (RF-Lambda RFLC313G27G37, 0.6-dB loss) by which optional probe signals can be reflected off of the cavity or the cavity mode noise can be read out. The  $TE_{01\delta}$  mode is characterized by monitoring the S21 parameter through the circulator using a Keysight N9915A microwave analyzer in network analyzer mode. The degree of loop-cavity coupling can be continuously adjusted via the loop position (e.g., translation stage) and stub tuner, with the reflected Lorentzian linewidth FWHM asymptotically approaching 140 kHz ( $Q \approx 2 \times 10^4$ ) and measuring about 230 kHz at critical coupling. Fine adjustments to the loop position are needed to recover critical coupling when the optically pumped N-V ensemble is resonant with the cavity. To verify the cavity measurements, we simulate the system with finite element methods using the COMSOL Multiphysics<sup>®</sup> electromagnetic wave module. The mode frequency and linewidth from these simulations are in excellent agreement with measurements, and further details are given in the Supplemental Material [24].

The cavity mode noise is measured with a Keysight N9915A microwave analyzer in spectrum analyzer mode. The adjustable resolution bandwidth  $B$  sets the frequency range over which the flat thermal noise is integrated, corresponding to a theoretical thermal noise floor of  $N_p = k_B T B$  with Boltzmann constant  $k_B$  and temperature  $T$ . For  $B = 30$  kHz at 300 K, this corresponds to a power level of  $-129$  dBm. The noise figure of the spectrum analyzer of 22.5 dB sets the actual floor to  $-106.5$  dBm. To operate well-above instrumentation noise, we use two low-noise amplifiers in series: the first with 55.7-dB gain and noise figure 0.75 dB (RF-Lambda RLNA02G04G60) and the second with 37.1-dB gain and noise figure 0.8 dB (RF-Lambda RLNA02G08G30). Together these elevated the thermal noise of the cavity mode to  $-42.8$  dBm. Precise determination of the noise floor is accomplished by averaging a few hundred traces to eliminate instantaneous phase fluctuations on the internal oscillator of the spectrum analyzer.

We first characterize the N-V cavity system to estimate the model parameters. With the spins unpolarized (laser off) and not resonant with the cavity, we measured the unloaded cavity mode frequency to be 2891 MHz with a linewidth of  $\gamma = 140$  kHz full width at half maximum (FWHM), corresponding to a quality factor of about  $2 \times 10^4$ . Introducing the coupling loop and critically coupling to the cavity increased the linewidth by a factor of 2. ODMR measurements over the entire diamond gave Gaussian-broadened linewidths of 290 kHz. Previous measurements of similar samples under controlled conditions to minimize the effects of strain and field gradients gave linewidths closer to 200 kHz, suggesting that these sources contribute to broadening in our N-V spin population.

Cooling occurs when the N-V spins are resonant with the cavity mode. At this resonance, strong coupling between the polarized spin ensemble and the cavity splits the cavity resonance into hybrid spin-cavity eigenmodes. We utilized this cavity splitting to locate the resonance frequency and quantify the amount of coupling for our system. The detuning between the N-V spins and the cavity mode ( $\Delta$ ) is controlled by keeping the cavity resonance fixed and scanning the spin transition frequency. Using a uniform magnetic field generated by three sets of orthogonal Helmholtz coil electromagnets aligned to the  $\langle 100 \rangle$  crystal axis, all four N-V orientations can be swept through the cavity resonance simultaneously.

The spin-cavity coupling is measured via the cavity mode splitting. A weak probe signal is reflected off of the cavity and the amplitude spectra (Fig. 3) are collected for a range of  $\Delta$  by means of microwave homodyne detection. In general, the  $^{14}\text{N}$ -induced hyperfine interaction splits the spin transition into three subensembles separated by roughly 2.15 MHz, resolvable in both our ODMR calibration and cavity reflectivity measurements. The splitting  $\delta\nu$  as the magnetic field shifts the spins through the cavity in Fig. 3 occurs at a distinct bias for each of the three subensembles. Combined with knowledge of the

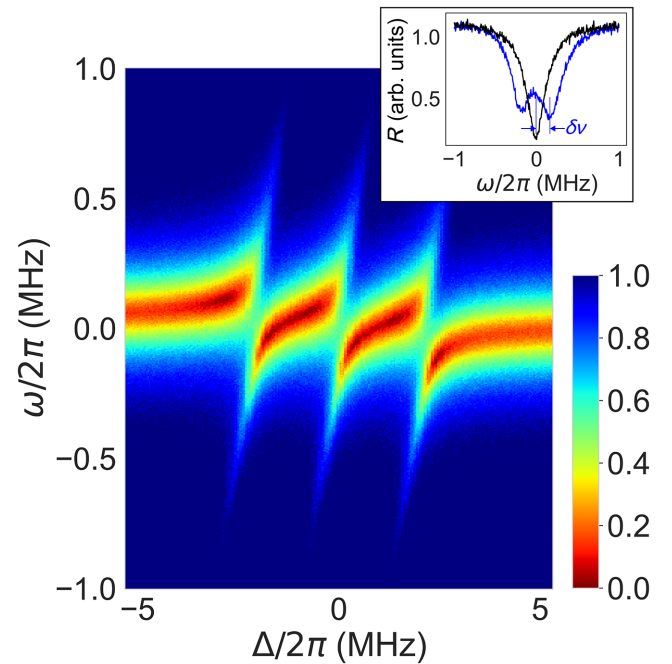


FIG. 3. The splitting  $\delta\nu$  due to the collective coupling of the spin ensemble to the cavity mode is measured by reflecting a weak probe at cavity detuning  $\omega$  as the N-V spin detuning  $\Delta$  is swept through the bare cavity resonance at 2895.3 MHz. The data shown here are for a laser pump power of 5.5 W distributed over the whole diamond. Three splittings are visible due to the  $^{14}\text{N}$  hyperfine interaction. The inset shows the middle splitting (red dashed line) compared with the bare cavity resonance.

ground-state spin polarization, this splitting ( $\delta\nu \approx 200$  kHz in Fig. 3) quantifies the collective coupling between the low-temperature spin bath and the cavity mode.

#### IV. RESULTS

Our main experimental result of fully continuous, spectrally resolved microwave cavity mode cooling is shown in Fig. 4. For a cw pump power of 3 W distributed over the whole diamond and critical output coupling, we report a maximum thermal noise reduction of  $-2.3 \pm 0.1$  dB, which corresponds to an effective temperature of the cavity output of  $150 \pm 5$  K when accounting for detection noise and bandwidth.

The cavity mode cooling measurement is conducted for a range of spin-cavity detunings  $\Delta$  but without a probe signal and with the input to the coupling loop circulator terminated. The spin-polarizing pump laser is kept on continuously throughout the experiment. Because the pump laser also heats the diamond through absorption (and thus the resonator through thermal contact), a sufficient amount of time for equilibration (i.e., a few minutes) is allowed after any changes to the pump power setpoint. The coupling loop position is then tuned to achieve near-critical coupling to the cavity mode. A three-stub tuner impedance matched the short (10 cm) coaxial feed from the coupling loop to the detection circuit. This circuit is made up of a low-loss circulator (isolator), two series low-noise high-gain amplifiers ( $N_{F_{\text{tot}}} < 0.8$  dB,  $G_{\text{tot}} \approx +93$  dB), and a spectrum analyzer with sufficiently low instrumentation noise. To reduce the effect of instantaneous measurement fluctuations due to phase noise on the spectrum analyzer

internal oscillator, 200 independent traces are averaged for each spin detuning.

Thermal noise power goes as  $N_P = k_B T B$ , where  $B$  represents the measurement bandwidth. In our case this is set by the spectrum analyzer resolution bandwidth that is fixed to  $B = 30$  kHz, corresponding to  $-129.2$  dBm at 290 K. The two-stage, low-noise amplifier further raised this noise floor to  $-42.8$  dBm, over 100 dB above the technical floor of the spectrum analyzer, while contributing negligible additional noise. We checked the dominance of thermal noise in our measurement by verifying the bandwidth dependence and agreement with theory (Supplemental Material [24]).

The spectral shape of the mode cooling is discerned through use of a sufficiently narrow detection bandwidth. Figure 4(a) clearly shows three well-resolved noise dips as each of the hyperfine subensembles become resonant with the cavity. A fit to our model, shown in Fig. 4(b), accurately reproduces the noise suppression for fixed  $\gamma = 2\pi \times 140$  kHz (as determined from reflectivity measurements) and free parameters  $g = 2\pi \times 197.7$  kHz (similar to the measured cavity splitting),  $r = 2\pi \times 229.0$  kHz (less than but similar to the ODMR broadening), and  $\kappa = 2\pi \times 185.1$  kHz (indicating slight overcoupling). A prefactor accounts for 1.35 dB of loss between the coupling loop and the detector.

The slices shown in Figs. 4(c) and 4(d) along the spin and microwave frequency axes, respectively, reveal the sensitivity to tuning mismatch and the cooling bandwidth. From Fig. 4(c), it is seen that the noise dips have a FWHM  $\approx 670$  kHz, roughly 2–3 times the spin ensembles inhomogeneous linewidth as measured from ODMR.

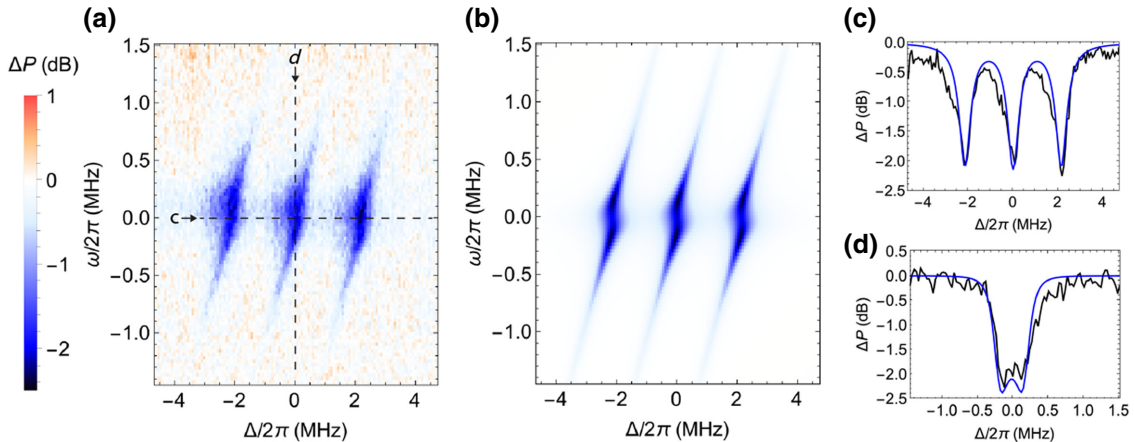


FIG. 4. Measured change in thermal noise on the cavity output and comparison with the model: (a) steady-state change in noise power (compared with no pump) at cavity microwave detuning  $\omega$  and N-V spin detuning  $\Delta$  for an optical pump power of 3 W and 30-kHz detection bandwidth, (b) model prediction [Eq. (2)] assuming a spin polarization  $P = 0.8$ , and parameters  $g = 2\pi \times 197.7$  kHz,  $\gamma = 2\pi \times 140$  kHz,  $r = 2\pi \times 229.0$  kHz, and  $\kappa = 2\pi \times 185.1$  kHz. Slices along the N-V spin detuning axis and microwave cavity output frequency axis are shown in (c) and (d), respectively, along with the theory prediction from (b). At this pump intensity we report a peak  $(-2.3 \pm 0.1)$ -dB reduction in thermal noise ( $150 \pm 5$  K) compared with an unpumped system.

For a single subensemble tuned to the cavity resonance [Fig. 4(d)], the microwave spectrum has a broad, flattened shape with a FWHM  $\approx 750$  kHz bandwidth. This is also seen in the model, represented by a solid line and using the same fit parameters as listed above, and indicates the onset of strong coupling. As the spin-cavity coupling is increased, the model predicts a splitting of the cavity mode noise suppression. Our reflectivity measurements suggest that we are on the verge of strong coupling (often designated as when the cavity splitting exceeds the linewidth), and thus we do not resolve a splitting in the cooling but only a broadening.

The effective cooling rate depends critically on the spin-cavity coupling  $g$  [Eq. (2)] as well as the spin polarization  $P$  [Eq. (2)] that sets the effective temperature of the  $N-V$  spin ensemble. Although the bare  $g$ , which is partly determined by  $N-V$ -center concentration and cavity mode overlap with the diamond, is not easily changed in our experimental system, we could control the optical pump intensity with a variable attenuator that had a direct impact on  $P$ . We varied the pump laser intensity over 2 orders of magnitude and measured its effect on the cavity mode splitting and mode temperature. The results (Fig. 5) display an increase in both cavity splitting and mode cooling with higher laser power followed by a leveling off at about 3 W or  $10^{-4}$ -mW/ $\mu\text{m}^2$  optical intensity.

We explain these phenomena through a two-level  $N-V$  rate model [26] including the competing effects of optical spin pumping and temperature-dependent  $T_1$  relaxation. The blue filled region in Fig. 5 indicates the results of a Monte Carlo simulation for the spin polarization using the above model with uncertainties from the literature and estimated for our sample. The correlation seen in Fig. 5 between the cavity mode splitting (i.e., spin-cavity coupling) and ground-state polarization is explained by the former depending on the number of emitters coherently interacting with the cavity mode. As the optically induced spin pumping rate of the  $N-V$  ensemble becomes comparable to the longitudinal relaxation rate ( $1/T_1$ ), the polarization begins to saturate (top plot of Fig. 5). As the excitation laser beam is spread over a diameter of about 5 mm, leading to pumping intensities ( $<10^{-4}$  mW/ $\mu\text{m}^2$ ) much smaller than the  $N-V$  saturation intensity (about 1 mW/ $\mu\text{m}$ ) [26], nonlinear processes such as photoionization and charge state conversion are negligible. The steady-state polarization reached here is lower than that achieved in single- $N-V$  experiments [26] (Supplemental Material [24]), but as spin polarization is exponentially related to spin temperature [27,28], the limited polarization does not preclude microwave mode cooling. The dashed green line shows the model prediction [Eq. (2)] with the fitted parameters from Fig. 4 and matches the data for high polarization but fails to capture the data at small polarizations. The blue dashed line shows a phenomenological model where the effective  $g$  varies with the square root

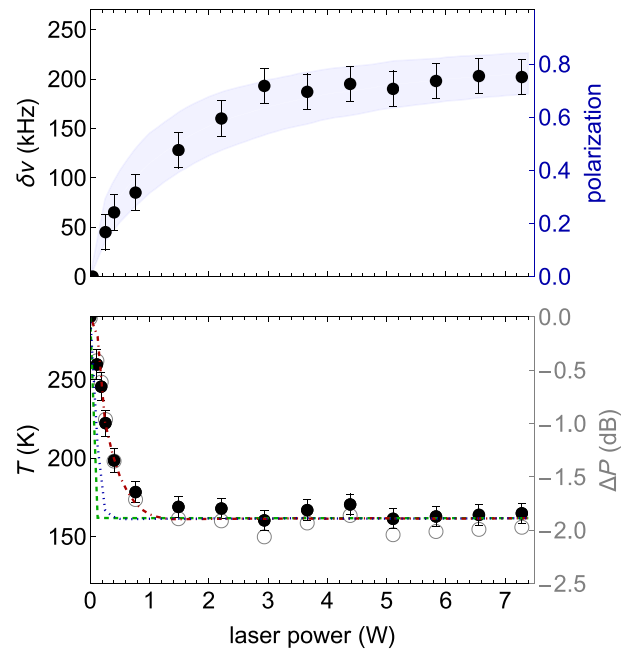


FIG. 5. Cavity mode splitting  $\delta\nu$  (top) and depth of cavity mode cooling (bottom) versus applied optical pump power. The mode splitting, itself a measure of spin-cavity coupling  $g$ , depends partly on the spin polarization generated by the pump laser. The predicted behavior from a model including temperature effects is shown by the blue region (Supplemental Material [24]). The bottom plot shows the inferred cavity mode temperature from measuring the noise power reduction on the output (black circles). Error bars indicate the standard error. The green dashed line shows the prediction by the linearized model, and the blue dash-dot line includes a phenomenological correction to the spin-cavity coupling.

of  $P$ , while the best agreement comes from assuming that  $g \propto P$ , shown as the red dash-dot line. Further theoretical work is required to understand this behavior at low optical pump powers.

The microwave mode cooling produced in the cavity can be transferred to a transmission line, producing nonthermal voltage power spectral density at a distance. A demonstration is shown in Fig. 6 where we vary the length of a coaxial microwave line from 0 to 6 m and measure the effective temperature from the noise power as before. We find that the cooling in the cavity band falls exponentially with cable length, with constant  $\alpha = 5.3$  m, consistent with the Ohmic loss in the line [29]. At a distance of 6 m we observe a reduction of 40 K, showing the potential of this technique for cooling on laboratory scales.

## V. OUTLOOK

The results presented here open a pathway to reducing noise in a range of applications as well as to achieving much lower temperatures. The latter could enable quantum technologies at ambient conditions. A number of routes to

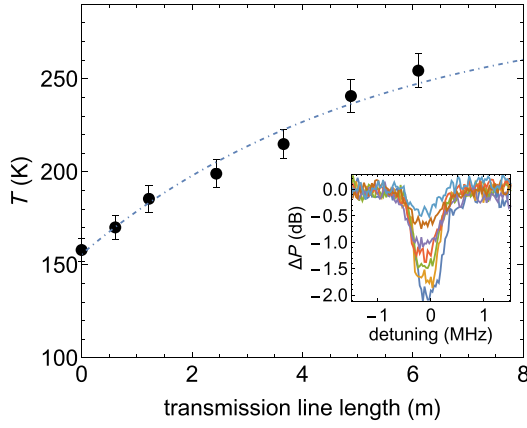


FIG. 6. Varying the length of the coaxial cable between the output of the cavity and the detector. We find that the rate of cooling decreases exponentially with a length constant of  $\alpha = 5.3$  m. Inset: spectrally resolved power reduction at varied cable lengths.

realizing lower temperatures exist. The number of spins could be increased by using a larger diamond sample or one with greater N- $V$  concentration. The effective spin-cavity coupling could be increased using cavity designs that concentrate the mode at the location of the ensemble while maintaining high  $Q$  [13]. Importantly, as our theoretical model reveals, cooling requires sufficient inhomogeneous broadening of the spins. Assuming that one starts with an underbroadened N- $V$  ensemble, tuning this inhomogeneous linewidth, for example with a magnetic field gradient, will allow one to optimize the thermal noise suppression. Finally, although in this system a magnetic field is used to tune the spins into resonance with a cavity mode relatively near the N- $V$  zero-field splitting, increased bias fields or the use of other spin defects could allow for cooling at other frequencies, thereby extending its usefulness. As it stands, the continuous cooling demonstrated in this work surpasses what is possible with thermoelectrically cooled systems, and offers strong potential for performance competitive with cryogenic systems in the future.

### ACKNOWLEDGMENTS

The authors would like to thank Danielle Braje and Erik Eisenach for helpful discussions. M.E.T. acknowledges support from the ARL ENIAC Distinguished Postdoctoral Fellowship. H.C. and D.E. acknowledge support from DARPA DRINQS. M.J.T. acknowledges support from the Army Research Laboratory Maryland-ARL Quantum Partnership program under Contract No. W911NF-19-2-0181 and the University of Maryland Quantum Technology Center.

### APPENDIX A: COOLING A MICROWAVE MODE WITH A N- $V$ ENSEMBLE

Nitrogen-vacancy centers in diamond contain a spin triplet that forms a  $V$  system, in which the two transitions are in the microwave band (approximately  $2\pi \times 2.87$  GHz). The states with  $J_z = \pm 1$  are the excited states and  $J_z = 0$  the ground state. In addition, naturally abundant  $^{14}\text{N}$  has a nuclear spin of 1, resulting in a triplet. The nuclear spins are merely an auxiliary system, and each electronic spin transition is split into three. Since the width of our cavity mode is much less than the separation of the hyperfine splitting, we use one of the transitions for cooling and treat the N- $V$  centers as a two-level system.

The Hamiltonian of the ensemble of N- $V$  centers and the microwave cavity mode is  $H$ , where

$$\frac{H}{\hbar} = \sum_j \Delta_j P_e^{(j)} + g_j (a\sigma_j^\dagger + \text{H.c.}).$$

Here  $P_e^{(j)}$  is the projector onto the upper level of the  $j$ th N- $V$  center, denoted  $|e, j\rangle$ ,  $\Delta_j$  is the detuning between spin  $j$  and the cavity mode,  $g_j$  is the interaction strength between spin  $j$  and the cavity mode, and  $a$  is the annihilation operator for the cavity mode. The cavity is single sided and damped through its single output coupling at rate  $\kappa$ . We denote the internal loss rate of the cavity by  $\gamma$ .

Room-temperature thermal noise flows into the mode at rate  $\gamma$  due to internal loss and at rate  $\kappa$  from the input-output coupling. However, it is only the noise at rate  $\gamma$  that represents unavoidable heating. To reach the lowest temperature when cooling the mode, we can turn off the output coupling.

Optical pumping of N- $V$  centers polarizes them such that the population is in the ground state. We deduce the temperature of the N- $V$  bath as a function of the polarization. Since the cooling will be achieved simply by coupling the mode to this cold bath, it is also useful to know what the average thermal occupation of the mode would be if it were at the temperature of the spins. This would be the number of photons in the mode if it were at thermal equilibrium with the spins.

The polarization of the N- $V$  centers (i.e., the length of the Bloch vector) is

$$P = |p_g - p_e| = |2p_g - 1| = |1 - 2p_e|, \quad (\text{A1})$$

where  $p_g, p_e$  are the populations of the ground state and excited states, respectively. The average number of photons in a resonator that is at the same temperature as an ensemble of spins with this polarization is

$$n_{\text{cold}} = \frac{1}{2} \left( \frac{1 - P}{P} \right), \quad (\text{A2})$$

and the temperature of the mode (and the spins) would be

$$T_{\text{cold}} = \frac{\hbar\omega/k_B}{\ln[1 + 1/n_{\text{cold}}]}, \quad (\text{A3})$$

where  $\omega$  is the frequency of the mode (in our case approximately  $2\pi \times 3$  GHz).

From Eq. (A2) we find that even if the spin polarization is only 70% ( $P = 0.7$ ) then the spin bath is at a temperature in which the mode would have only about 0.2 photons. The spin ensemble is thus a very cold bath for the mode.

The pump laser polarizes the spins, acting against the intrinsic damping rate of the spins that would otherwise thermalize them at the ambient temperature. The polarizing rate depends on the laser power, and must be at least comparable to the intrinsic damping rate to keep the spins cold (sufficiently well polarized).

One might think that the cooling mechanism would work as follows. The mode is coupled to the spins via a unitary interaction that would usually cause a cycling of energy between the mode and the spins at the Rabi frequency given by the collective coupling rate. The cooling of the spins by the laser sucks this energy out of the spins at a similar or higher rate, thus suppressing the oscillations. In that case the rate at which the laser cools the spins would determine the rate of energy extraction from the mode. Somewhat surprisingly, this is not the mechanism for cooling, at least only indirectly.

To understand what sets the cooling rate for the cavity mode, it is useful first to note that energy transferred to the spins from the mode is spread across the spins. Since there are  $10^{14}$  spins, the amount of energy transferred to each spin is extremely small. As a result, the rate at which the laser extracts energy from each spin can be very much smaller than the rate at which energy is transferred from the mode to the spin ensemble.

It is useful now to consider how a bath of oscillators takes energy out of a system irreversibly. The standard model of a thermal bath is an ensemble of oscillators whose frequencies form a near continuum with an essentially constant number of oscillators per unit frequency. This results in a very simple ‘‘Markovian’’ dynamics for the system in which the damping is given by rate equations. This is only true if the density of oscillators per unit frequency is flat (up to some very high frequency). If the bath has a spectral density of oscillators that is Lorentzian then it has been shown in Refs. [22,23,30] that the dynamics induced in the system is identical to that induced by coupling the system to a single (fictitious) oscillator that is itself coupled to a Markovian bath. The damping rate for the fictitious oscillator is the width of the Lorentzian spectrum for the bath.

Since the spins in the ensemble have very low excitation, they are well approximated by harmonic oscillators. The inhomogeneous spread of the spins therefore acts in

the same way as the spectral distribution of an oscillator bath, and thus produces an irreversible decay from the system into the ensemble. Admittedly, the frequency distribution of the spins is a Gaussian rather than a Lorentzian, but if we assume that treating it as a Lorentzian is a reasonable approximation, the spin bath is equivalent to coupling the mode to a fictitious oscillator in which this oscillator is damped at a rate given by the inhomogeneous broadening of the spins. It is therefore the inhomogeneous broadening that sets the rate at which energy is irreversibly extracted from the mode.

First we write down the quantum Langevin equations (input and output equations) for the mode, including the coupling to the spins, and then move to the equivalent mode that contains the fictitious oscillator. The Langevin equations are [19,20]

$$da = \left[ -\frac{\kappa + \gamma}{2}a - i \sum_j g_j \sigma_j \right] dt + \sqrt{\kappa} da_{\text{in}} + \sqrt{\gamma} db_{\text{in}}, \quad (\text{A4})$$

$$d\sigma_j = -\left( \frac{q}{2} + i\Delta_j \right) \sigma_j + ig_j (P_e^{(j)} - P_g^{(j)}) adt + \sqrt{q} (P_e^{(j)} - P_g^{(j)}) dc_{\text{in}}^{(j)}. \quad (\text{A5})$$

Here we have enforced the rotating-wave approximation for the interaction between the mode and the spins, and the laser cooling of the spins is modeled by a damping for the spins at rate  $q$ . The correlation functions for the input field  $a_{\text{in}}$  are

$$\langle a_{\text{in}}^\dagger(t) a_{\text{in}}(t') \rangle = n_T \delta(t' - t), \quad (\text{A6})$$

$$\langle a_{\text{in}}(t) a_{\text{in}}^\dagger(t') \rangle = (n_T + 1) \delta(t' - t). \quad (\text{A7})$$

Those for  $b_{\text{in}}$  are the same, and those for  $c_{\text{in}}$  are obtained merely by replacing  $n_T$  with  $n_{\text{cold}}$  in Eq. (A7).

We now write down the equivalent model in which the spin bath is replaced by a single fictitious oscillator as described above. This model is [22,23,30].

$$da = \left[ -\frac{\kappa + \gamma}{2}a - igf \right] dt + \sqrt{\kappa} da_{\text{in}} + \sqrt{\gamma} db_{\text{in}}, \quad (\text{A8})$$

$$df = -\left( \frac{r}{2} - i\Delta \right) f dt + igadt + \sqrt{r} dc_{\text{in}}.$$

Here  $f$  is the mode operator for the fictitious oscillator,  $r$  is the width of the (assumed Lorentzian) frequency distribution of the spins, and  $g = \sqrt{\sum_j g_j^2}$  is the collective interaction with the spin bath.



One way to determine the steady-state energy of the cooled mode is to derive the equations of motion for the second moments of  $a$  and  $f$ . These are

$$\begin{aligned} dn &= d(a^\dagger a) = da^\dagger a + a^\dagger da + da^\dagger da \\ &= \left[ -\frac{K}{2}ndt + igf^\dagger dt + (\sqrt{\kappa}da_{\text{in}}^\dagger + \sqrt{\gamma}db_{\text{in}}^\dagger)a + \text{H.c.} \right] + Kn_T dt \\ &= -K[n - n_T]dt + \left[ igf^\dagger adt + (\sqrt{\kappa}da_{\text{in}}^\dagger + \sqrt{\gamma}db_{\text{in}}^\dagger)a + \text{H.c.} \right], \end{aligned} \quad (\text{A9})$$

$$\begin{aligned} d(f^\dagger a) &= df^\dagger a + f^\dagger da + df^\dagger da \\ &= \left\{ -\left[ \frac{r}{2} + i\Delta \right]f^\dagger dt + iga^\dagger dt + \sqrt{r}dc_{\text{in}}^\dagger \right\} a + f^\dagger \left[ -\frac{K}{2}adt - igfdt + (\sqrt{\kappa}da_{\text{in}}^\dagger + \sqrt{\gamma}db_{\text{in}}^\dagger)a \right] \\ &= -\left[ \frac{K+r}{2} + i\Delta \right]f^\dagger adt + iga^\dagger adt - igf^\dagger f + \sqrt{\kappa}da_{\text{in}}f_j^\dagger + \sqrt{\gamma}db_{\text{in}}f^\dagger + \sqrt{r}dc_{\text{in}}^\dagger a, \end{aligned} \quad (\text{A10})$$

$$d(f^\dagger f) = df^\dagger f + f^\dagger df + df^\dagger df = -rf^\dagger fdt + i(a^\dagger gf - gf^\dagger a)dt + rn_{\text{cold}}dt + \sqrt{r}dc_{\text{in}}^\dagger f + \sqrt{r}dc_{\text{in}}f^\dagger, \quad (\text{A11})$$

with  $K \equiv \kappa + \gamma$ . We now solve these for the steady state. Setting the derivatives to zero we have

$$\bar{n} = n_T + \frac{i}{K}[s - s^*], \quad (\text{A12})$$

$$\left( \frac{K+r}{2} + i\Delta \right) s = ig^2 \bar{n} - iQ, \quad (\text{A13})$$

$$Q = g^2 n_{\text{cold}} - \frac{ig^2}{r}[s - s^*], \quad (\text{A14})$$

where we have defined

$$\bar{n} = \langle n \rangle, \quad s = g\langle f^\dagger a \rangle, \quad Q = g^2 \langle f^\dagger f \rangle. \quad (\text{A15})$$

We first eliminate  $Q$  by substituting Eq. (A14) into Eq. (A13):

$$\left( \frac{K+r}{2} + i\Delta \right) s = ig^2(\bar{n} - n_{\text{cold}}) - \frac{g^2}{r}[s - s^*]. \quad (\text{A16})$$

Writing  $s - s^*$  in the form

$$s - s^* = \frac{2[(K+r)/2]}{[(K+R)/2]^2 + \Delta^2} \left[ ig^2(\bar{n} - n_{\text{cold}}) - \frac{g^2}{r}(s - s^*) \right]. \quad (\text{A17})$$

We combine the  $s - s^*$  terms and rearrange to obtain

$$s - s^* = i \frac{4g^2 L_{K+r}(\Delta)/(K+r)}{1 + [4g^2/(K+r)]L_{K+r}(\Delta)/r} (\bar{n} - n_{\text{cold}}), \quad (\text{A18})$$

where  $L_{K+r}(\Delta) = [(K+r)/2]^2 / \{ [(K+r)/2]^2 + \Delta^2 \}$  is the Lorentzian with a FWHM of  $K+r$  and a maximum of 1. We can simplify the equation using

$R = 4g^2 L_{K+r}(\Delta)/(K+r)$ , the adiabatic population transfer rate:

$$s - s^* = i \frac{rR}{r+R} (\bar{n} - n_{\text{cold}}). \quad (\text{A19})$$

Substituting this into the above yields

$$\bar{n} = n_T - \frac{1}{K} \frac{rR}{r+R} (\bar{n} - n_{\text{cold}}). \quad (\text{A20})$$

This expression is a weighted average of the occupation numbers of the hot and cold baths,  $n_T$  and  $n_{\text{cold}}$ . Rearranging gives,

$$K(\bar{n} - n_T) = (r|R)(\bar{n} - n_{\text{cold}}), \quad (\text{A21})$$

where  $a||b = ab/(a+b)$  is the series transfer rate which is the same as the parallel resistance.

Note that Eq. (A21) has an intuitive interpretation; the heating  $K(\bar{n} - n_T)$  equals the cooling  $(r|R)(\bar{n} - n_{\text{cold}})$ ; the cooling rate  $(r|R)$  is limited by whether either the damping rate  $r$  or the population transfer  $R$  between the cavity and spins is slower. We define the cooling rate  $\Gamma = r|R$ .

The cooling rate  $\Gamma$  approaches the inhomogeneous broadening  $(r)$  when  $R \gg r$ , or, equivalently,

$$g \gg \sqrt{r(K+r)}. \quad (\text{A22})$$

If the spins are also heating at an appreciable rate  $\nu$  to the thermal occupation  $n_T$ , the cooled cavity photon number

will be

$$\bar{n} = \frac{[R'/(R' + r')]rn_{\text{cold}} + \{[R'/(R' + r')]v + K\}n_T}{R'r'/(R' + r') + K}, \quad (\text{A23})$$

where  $r' = r + v$  and  $R' = 4g^2 L_{K+r'}(\Delta)/(K + r')$ .

We also note that, for the resonant case ( $\Delta = 0$ ),

$$\frac{K}{\Gamma} = \frac{K}{r} \left( \frac{r(K + r)}{4g^2} + 1 \right) = \frac{\kappa + \gamma}{r} \left( \frac{r(\kappa + \gamma + r)}{4g^2} + 1 \right). \quad (\text{A24})$$

When the output coupling goes to zero, which gives the best cooling, then

$$\frac{K}{\Gamma} = \left( \frac{\gamma}{r} + \frac{\gamma(\gamma + r)}{4g^2} \right). \quad (\text{A25})$$

## APPENDIX B: OUTPUT POWER SPECTRUM FROM A SINGLE-SIDED CAVITY COOLED VIA A COLD DAMPED OSCILLATOR

We start with the model of the dynamics in which the cavity mode is coupled to a fictitious damped oscillator, given in Appendix A [Eq. (A8)]:

$$da = - \left[ \frac{\kappa + \gamma}{2} + i\Delta \right] adt - igfdt + \sqrt{\kappa} da_{\text{in}} + \sqrt{\gamma} db_{\text{in}}, \quad (\text{B1})$$

$$df = - \left[ \frac{r}{2} \right] fdt - igadt + \sqrt{r} dc_{\text{in}}. \quad (\text{B2})$$

Here  $\kappa$  is the input-output coupling rate,  $\gamma$  is the internal loss rate,  $r$  is the effective cooling rate of the cold

fictitious oscillator, and  $g$  is the collective coupling to the spin ensemble. We now transform these equations to frequency space, giving

$$-i\omega A = - \left[ \frac{\kappa + \gamma}{2} + i\Delta \right] A - igF + \sqrt{\kappa} \tilde{a}_{\text{in}} + \sqrt{\gamma} \tilde{b}_{\text{in}}, \quad (\text{B3})$$

$$-i\omega F = - \left[ \frac{r}{2} \right] F - igA + \sqrt{r} \tilde{c}_{\text{in}}. \quad (\text{B4})$$

We write these in matrix form and calculate its inverse to determine the frequency-space solution for the mode operator:

$$A = \frac{(r/2 - i\omega)(\sqrt{\kappa} \tilde{a}_{\text{in}} + \sqrt{\gamma} \tilde{b}_{\text{in}}) - ig\sqrt{r} \tilde{c}_{\text{in}}}{(r/2 - i\omega)[(\kappa + \gamma)/2 - i(\omega - \Delta)] + g^2}.$$

Using the input and output relations in Refs. [19,31], the field output from the cavity mode is

$$\begin{aligned} a_{\text{out}}(\omega) &= \sqrt{\kappa} A - a_{\text{in}}(\omega) \\ &= \frac{\sqrt{\kappa\gamma}(r/2 - i\omega)\tilde{b}_{\text{in}} - i\sqrt{\kappa r}g\tilde{c}_{\text{in}}}{(r/2 - i\omega)[(\kappa + \gamma)/2 - i(\omega - \Delta)] + g^2} \\ &\quad + \left[ \frac{(r/2 - i\omega)[(\kappa - \gamma)/2 + i(\omega - \Delta)] - g^2}{(r/2 - i\omega)[(\kappa + \gamma)/2 - i(\omega - \Delta)] + g^2} \right] \tilde{a}_{\text{in}}. \end{aligned} \quad (\text{B5})$$

To find the power spectrum of the output field  $S(\omega)$ , we use the autocorrelation function in frequency space:

$$\langle a_{\text{out}}^\dagger(\omega) a_{\text{out}}(\omega') \rangle = S(\omega) \delta(\omega + \omega'); \quad (\text{B6})$$

then

$$S(\omega) = \frac{\langle a_{\text{out}}^\dagger(-\omega) a_{\text{out}}(\omega) \rangle}{\delta(\omega - \omega')} = n_T + \frac{\kappa r g^2 (n_c - n_T)}{[r^2/4 + \omega^2][(\kappa + \gamma)^2/4 + (\omega - \Delta)^2] + g^4 + g^2[r(\kappa + \gamma)/2 - 2\omega(\omega - \Delta)]} \quad (\text{B7})$$

with

$$S(\omega)|_{\Delta=0} = n_T + \frac{\kappa r g^2 (n_c - n_T)}{[r^2/4 + \omega^2][(\kappa + \gamma)^2/4 + \omega^2] + g^4 + g^2[r(\kappa + \gamma)/2 - 2\omega^2]}, \quad (\text{B8})$$

$$S(0)|_{\Delta=0} = n_T - (n_T - n_c) \frac{\kappa r g^2}{[r(\kappa + \gamma)/4 + g^2]^2} = n_T - (n_T - n_c) \frac{\kappa r}{g^2 [1 + r(\kappa + \gamma)/4g^2]^2} \quad (\text{B9})$$

the minimized output powers on resonance ( $\Delta = 0$ ) where the spectrum is coldest.

The minimum is  $\omega = 0$  unless

$$g^2 > \frac{r^2}{8} + \frac{(\kappa + \gamma)^2}{8}, \quad (\text{B10})$$

and at  $\omega = 0$  we have

$$S(0) = n_T - (n_T - n_c) \frac{\kappa r}{g^2[1 + r(\kappa + \gamma)/4g^2]^2}. \quad (\text{B11})$$

The value of  $\kappa$  for which this is minimum is

$$k = \gamma + \frac{4g^2}{r}. \quad (\text{B12})$$

- [1] S. Krinner, S. Storz, P. Kurpiers, P. Magnard, J. Heinsoo, R. Keller, J. Lütolf, C. Eichler, and A. Wallraff, Engineering cryogenic setups for 100-qubit scale superconducting circuit systems, *EPJ Quantum Technol.* **6**, 2 (2019).
- [2] S. Putz, D. O. Krimer, R. Amsüss, A. Valookaran, T. Nöbauer, J. Schmiedmayer, S. Rotter, and J. Majer, Protecting a spin ensemble against decoherence in the strong-coupling regime of cavity QED, *Nat. Phys.* **10**, 720 (2014).
- [3] P. Krantz, M. Kjaergaard, F. Yan, T. P. Orlando, S. Gustavsson, and W. D. Oliver, A quantum engineer's guide to superconducting qubits, *Appl. Phys. Rev.* **6**, 021318 (2019).
- [4] Shirin Montazeri, Wei-Ting Wong, Ahmet H. Coskun, and Joseph C. Bardin, Ultra-low-power cryogenic sige low-noise amplifiers: Theory and demonstration, *IEEE Trans. Microw. Theory Tech.* **64**, 178 (2016).
- [5] Paul D. Lett, Richard N. Watts, Christoph I. Westbrook, William D. Phillips, Phillip L. Gould, and Harold J. Metcalf, Observation of Atoms Laser Cooled below the Doppler Limit, *Phys. Rev. Lett.* **61**, 169 (1988).
- [6] A. M. Kaufman, B. J. Lester, and C. A. Regal, Cooling a Single Atom in an Optical Tweezer to Its Quantum Ground State, *Phys. Rev. X* **2**, 041014 (2012).
- [7] B. E. King, C. S. Wood, C. J. Myatt, Q. A. Turchette, D. Leibfried, W. M. Itano, C. Monroe, and D. J. Wineland, Cooling the Collective Motion of Trapped Ions to Initialize a Quantum Register, *Phys. Rev. Lett.* **81**, 1525 (1998).
- [8] H. Rohde, S. T. Gulde, C. F. Roos, P. A. Barton, D. Leibfried, J. Eschner, F. Schmidt-Kaler, and R. Blatt, Sympathetic ground-state cooling and coherent manipulation with two-ion crystals, *J. Opt. B: Quantum Semiclass. Opt.* **3**, S34 (2001).
- [9] C. Metzger and K. Karrai, Cavity cooling of a microlever, *Nature* **432**, 1002 (2004).
- [10] A. Schliesser, P. Del'Haye, N. Nooshi, K. J. Vahala, and T. J. Kippenberg, Radiation Pressure Cooling of a Micromechanical Oscillator Using Dynamical Backaction, *Phys. Rev. Lett.* **97**, 243905 (2006).
- [11] Hao Wu, Shamil Mirkhanov, Wern Ng, and Mark Oxborrow, Bench-Top Cooling of a Microwave Mode Using an Optically Pumped Spin Refrigerator, *Phys. Rev. Lett.* **127**, 053604 (2021).
- [12] Wern Ng, Hao Wu, and Mark Oxborrow, Quasi-continuous cooling of a microwave mode on a benchtop using hyperpolarized NV- diamond, *Appl. Phys. Lett.* **119**, 234001 (2021).
- [13] Hyeonrak Choi and Dirk Englund, Ultrastrong magnetic light-matter interaction with cavity mode engineering, Preprint [ArXiv:2108.13266](https://arxiv.org/abs/2108.13266) (2021).
- [14] Marcus W. Doherty, Neil B. Manson, Paul Delaney, Fedor Jelezko, Jörg Wrachtrup, and Lloyd C. L. Hollenberg, The nitrogen-vacancy colour centre in diamond, *Phys. Rep.* **528**, 1 (2013).
- [15] E. R. Eisenach, J. F. Barry, M. F. O'Keefe, J. M. Schloss, M. H. Steinecker, D. R. Englund, and D. A. Braje, Cavity-enhanced microwave readout of a solid-state spin sensor, *Nat. Commun.* **12**, 1357 (2021).
- [16] Andrew M. Edmonds, Connor A. Hart, Matthew J. Turner, Pierre-Olivier Colard, Jennifer M. Schloss, Kevin Olsson, Raisa Trubko, Matthew L. Markham, Adam Rathmill, Ben Horne-Smith, Wilbur Lew, Arul Manickam, Scott Bruce, Peter G. Kaup, Jon C. Russo, Michael J. DiMario, Joseph T. South, Jay T. Hansen, Daniel J. Twitchen, and Ronald Walsworth, Characterisation of CVD diamond with high concentrations of nitrogen for magnetic-field sensing applications, *Mater. Quantum Technol.* **1**, 025001 (2021).
- [17] Yoshihisa Yamamoto and Atac Imamoglu, *Mesoscopic Quantum Optics* (Wiley, 1999).
- [18] Klaus Hepp and Elliott H. Lieb, On the superradiant phase transition for molecules in a quantized radiation field: The Dicke Maser model, *Ann. Phys.* **76**, 360 (1973).
- [19] C. W. Gardiner and M. J. Collett, Input and output in damped quantum systems: Quantum stochastic differential equations and the master equation, *Phys. Rev. A* **31**, 3761 (1985).
- [20] K. Jacobs, *Quantum Measurement Theory and Its Applications* (Cambridge University Press, Cambridge, 2014).
- [21] Kurt Jacobs, Hendra I. Nurdin, Frederick W. Strauch, and Matthew James, Comparing resolved-sideband cooling and measurement-based feedback cooling on an equal footing: Analytical results in the regime of ground-state cooling, *Phys. Rev. A* **91**, 043812 (2015).
- [22] A. Imamoglu, Stochastic wave-function approach to non-Markovian systems, *Phys. Rev. A* **50**, 3650 (1994).
- [23] B. M. Garraway, Nonperturbative decay of an atomic system in a cavity, *Phys. Rev. A* **55**, 2290 (1997).
- [24] See Supplemental Material at <http://link.aps.org/supplemental/10.1103/PhysRevApplied.20.014033> for additional details regarding the theoretical analysis and experimental methods.
- [25] D. P. L. Aude Craik, P. Kehayias, A. S. Greenspon, X. Zhang, M. J. Turner, J. M. Schloss, E. Bauch, C. A. Hart, E. L. Hu, and R. L. Walsworth, *et al.*, Microwave-Assisted Spectroscopy Technique for Studying Charge State in Nitrogen-Vacancy Ensembles in Diamond, *Phys. Rev. Appl.* **14**, 014009 (2020).
- [26] A. Dréau, M. Lesik, L. Rondin, P. Spinicelli, O. Arcizet, J.-F. Roch, and V. Jacques, Avoiding power broadening in optically detected magnetic resonance of single NV defects for enhanced dc magnetic field sensitivity, *Phys. Rev. B* **84**, 195204 (2011).
- [27] D. M. Toyli, D. J. Christle, A. Alkauskas, B. B. Buckley, C. G. Van de Walle, and D. D. Awschalom, Measurement and Control of Single Nitrogen-Vacancy Center Spins above 600 k, *Phys. Rev. X* **2**, 031001 (2012).
- [28] A. Jarmola, V. M. Acosta, K. Jensen, S. Chemerisov, and D. Budker, Temperature- and Magnetic-Field-Dependent

- Longitudinal Spin Relaxation in Nitrogen-Vacancy Ensembles in Diamond, [Phys. Rev. Lett. \*\*108\*\*, 197601 \(2012\)](#).
- [29] Dimitrios C. Agouridis, Thermal noise of transmission lines: A generalized solution, [IEEE Trans. Instrum. Meas. \*\*IM-36\*\*, 132 \(1987\)](#).
- [30] B. J. Dalton, Stephen M. Barnett, and B. M. Garraway, Theory of pseudomodes in quantum optical processes, [Phys. Rev. A \*\*64\*\*, 053813 \(2001\)](#).
- [31] M. J. Collett and C. W. Gardiner, Squeezing of intracavity and traveling-wave light fields produced in parametric amplification, [Phys. Rev. A \*\*30\*\*, 1386 \(1984\)](#).